Relative luminosity at pp2pp run 2009

I. Alekseev, L. Koroleva, B. Morozov, D. Svirida

ITEP, Moscow

February 13, 2013

Abstract

This note is dedicated to the relative luminosity of pp2pp Run in 2009. Several different sources of the luminosity information were checked. Finally BBC coincidence was found to be the best one. We estimate the systematic error of the angular independent part of the transverse double spin asymmetry $\delta\frac{A_{NN}+A_{SS}}{2}$ due to the normalization uncertainty, to be $8.4 \cdot 10^{-4}$.

Contents

1 Introduction

Unlike the single spin asymmetry analysis where we do not need external normalization to get the result, because of its pure cosine angular dependence, relative luminosity of all 4 bunch spin combinations is required to get the values of the double spin asymmetries. We also can not rely on the luminosity normalization method developed for the main portion of STAR 2009 run [1], because pp2pp running was performed with very different beam optics and luminosity conditions and because very small values of double spin asymmetries require more precise relative luminosity measurements.

1.1 Definitions

This note will use the following three *independent* luminosity ratios:

$$R_2 = \frac{L^{++} + L^{--}}{L}, \qquad R_B = \frac{L^{++} + L^{+-}}{L}, \qquad R_Y = \frac{L^{++} + L^{-+}}{L}, \tag{1}$$

where L^{BY} are the counts with colliding bunch polarization combination $B, Y = +$ or $-$ and $L = L^{++} + L^{+-} + L^{-+} + L^{--}$ are total counts of the monitoring subsystem. These ratios could be interpreted as connected to double spin asymmetry (R_2), blue and yellow single spin asymmetries (R_B and R_Y). As it is shown in the appendix A the main contribution to the double spin asymmetry systematic error comes from R_2 and $\delta\frac{A_{NN}+A_{SS}}{2} \approx 2 \cdot \delta R_2$.

1.2 Subsystems

WCM - RHIC Wall Current Monitor. This is the accelerator system, measuring bunch per bunch current for each ring. The data is stored in the C-AD database and can be retrieved for each fill. We used proper bunch intensity products to obtain luminosity for each pair of the colliding bunches.

BBC - the STAR Beam-Beam Counters. These are the detectors of hexagonal plastic scintillator tiles, placed around the beam pipe on each side of the main detector. Inner 18 tiles on each side were connected to 2×16 scaler inputs. The layout showing tile to scaler input assignment is shown in fig. 1.

VPD - the STAR Vertex Position Detector. These are the detectors placed behind BBC close to the beam pipe.

ZDC - the STAR Zero Degree Calorimeter. These are the detectors placed after DX dipole to measure neutral particles with high rapidity.

1.3 Scalers

STAR scaler boards [2] have 24 inputs and from the user point of view could be considered as a memory array of 2^{24} 64-bit cells. Each RHIC bunch crossing a cell with the address corresponding to its 24 inputs is incremented. So in each board we have 2^{24} scalers counting separately each input bit combination. The 8 most significant input bits have the same assignment for all boards - 7 bits provide bunch number and one bit is BBC inner tiles coincidence. This note is based mostly on the information obtained by the scaler boards 6, 11 and 12, which were reset at the beginning of each run and read out at the end. Boards 11 and 12 count individual BBC tiles as in fig. 1. Inputs assignment of the board 6 is given in tab. 1.

2 Scaler data digital consistency checks

The signal from BBC timed coincidence was connected to several scaler inputs. Tab. 2 gives the total sum of the counts of the corresponding scalers for the 4 fills of dedicated pp2pp running. We see that, though counting of this signal when it is connected to different inputs of the same board is perfect, it is not so for different boards. The difference is more than 2%.

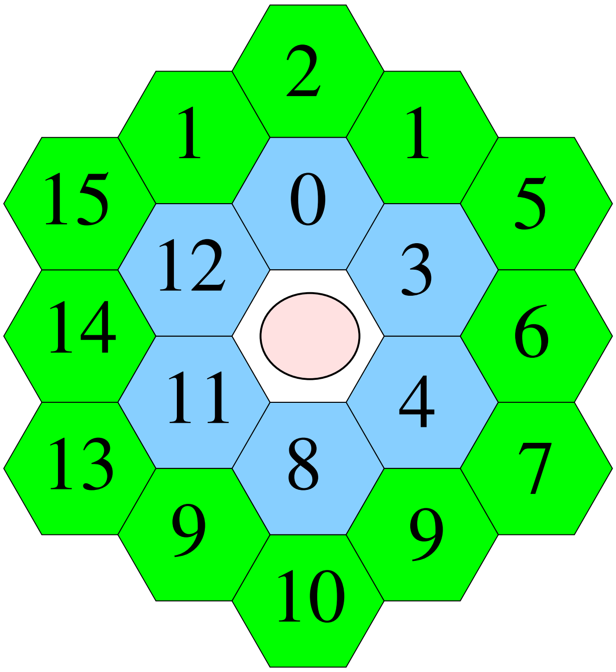

Figure 1: BBC tiles looking from the IP. Numbers represent tiles assignment to scaler boards 11 (east) and 12 (west) inputs.

Table 1: Board 6 input assignment

Bit	Assignment
0	VPD east hit
1	VPD west hit
2	VPD timed coincidence
3	BBC timed coincidence
4	BBC east-west time difference bit 0 out of the 4 its most significant bits
5	BBC east-west time difference bit 1 out of the 4 its most significant bits
6	BBC east-west time difference bit 2 out of the 4 its most significant bits
7	BBC east-west time difference bit 3 out of the 4 its most significant bits
8	BBC timed coincidence
9	ZDC east hit
10	ZDC west hit
11	ZDC timed coincidence
12	ZDC front east hit
13	ZDC front west hit
14	BBC east hit
15	BBC west hit
16	BBC timed coincidence

Table 2: Counting of the BBC coincidence signal by different boards

Board	Input	Sum over 4 fills
6	3	455 872 123
6	8	455 872 123
6	16	455 872 123
10	16	444 016 673
11	16	451 481 586
12	16	449 920 444

Another test for consistency can be performed looking at the counts for the cases, when we see coincidence bit for a certain subsystem while there is no hit in one or both of its arms. Though it is possible that when hits in both east and west arms are present they produce no coincidence due to the time difference, it is digitally forbidden to have coincidence when one of its components or even both are absent. Total counts for such behavior during the 4 fills are presented in tab. 3. While BBC and ZDC show tolerable level of illegal counts, the percent of illegal counts for VPD looks unreasonably high.

Table 3: Illegal signal combinations summed over 4 dedicated pp2pp fills

Detector	Correct coincidence	Forbidden coincidence	%
(CEW)	(111)	(100)+(101)+(110)	
BBC	452 938 208	2 933 915	0.6%
ZDC	2 933 915	169	0.006%
VPD	33 961 756	4 347 022	13%

The reason of such behavior is most likely in poor timing of the coincidence signals relative to the RHIC clock. This is illustrated in fig. 2, where BBC counts are shown as a function of bunch number. The top distribution shows events when the coincidence was accomplished by both east and west hits as one should naturally expect. The distribution in the bottom contains events where only the coincidence bit was present with neither east nor west hits. One can easily see that the bottom distribution is one bunch crossing delayed compared to the natural distribution on top[1]. The effect can happen when the coincidence signal is sometimes too long or late and leaks into the next bunch crossing.

As a conclusion we shall consider the percent of logically forbidden counts for VPD as too high and we will not use this detector for relative luminosity calculations. Instead we will use BBC and ZDC coincidence counts accompanied by signals on both sides (CEW=111) as the only *true* coincidence counts.

3 Comparison of various sources

3.1 WCM

WCM signal, measuring individual bunch currents, could be an ideal tool for relative luminosity because of its obvious spin independence. Unfortunately luminosity of the collisions depends not

[1]One can find more examples like this in fig. 2(4,5,6) and fig. 3(5) of [1]

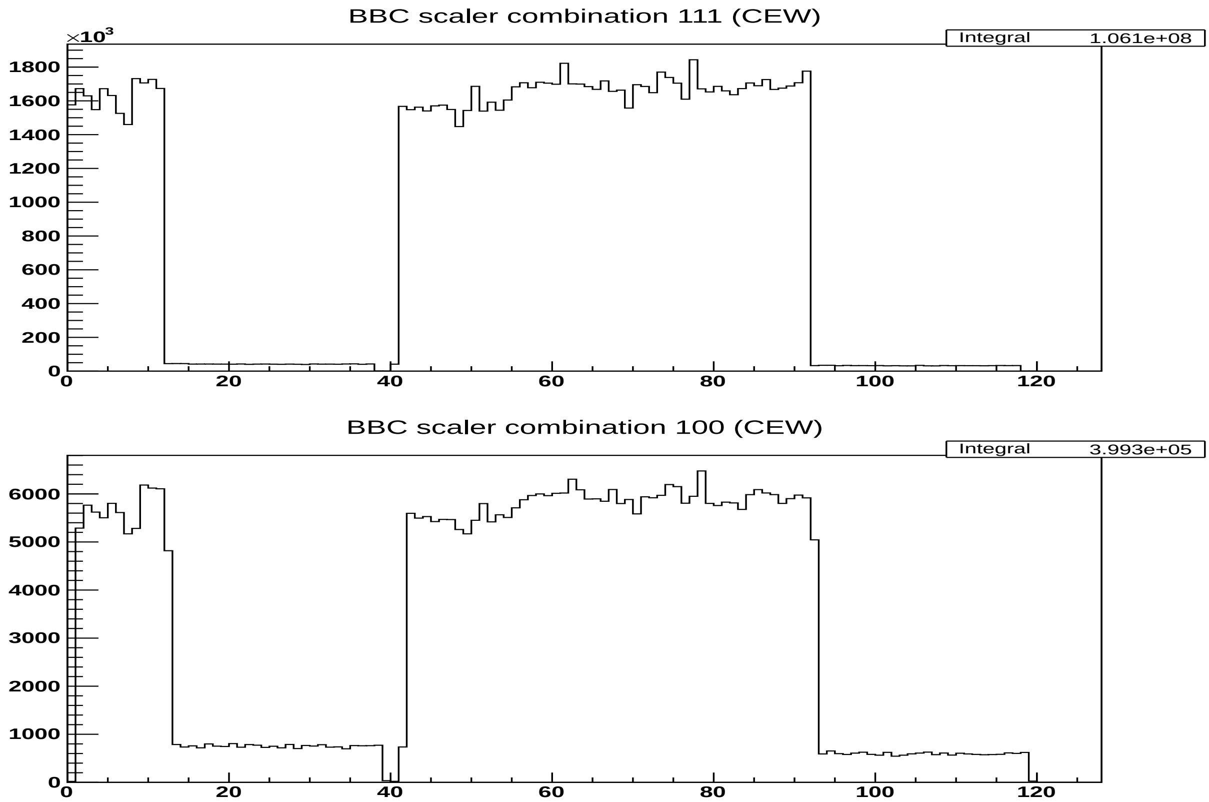

Figure 2: BBC coincidence counts as a function of the bunch number: both east and west bits are present (top) neither east or west bits are present (bottom).

only on the colliding bunch currents but also on the bunch shapes and the impact parameters. Table 4 shows bunch to bunch luminosity variation (ratio of RMS to mean) in %% for BBC and WCM data for the four pp2pp fills. One can see that with the exception of the fill 11020, where all bunches look to be of the same shape and have the same trajectory, variation for BBC measurement is significantly larger than that for WCM. In other words, the WCM product does not correctly reflect the variation of the luminosity and can not be used as luminosity monitor.

Table 4: Variation of bunch to bunch luminosity measured by BBC and WCM

Fill	BBC	WCM
11020	5 %	5 %
11026	26 %	16 %
11030	16 %	10 %
11032	14 %	8 %

3.2 ZDC

The bunch per bunch ratio of ZDC to BBC counts is presented in fig. 3 fitted by a constant. No clear bunch to bunch dependence is observed. We also don't see any knocked out bunches worth skipping. Another test is shown in fig. 4 where the same data points are shown as a function of BBC counts, i.e bunch luminosity. The observed luminosity dependence looks very small compared to the luminosity range we have. It could be also due to no corrections for accidentals and multiples applied for this test, (see [1]) though the effect of these corrections would be very small, as we worked at low luminosity. Even for a single BBC arm we had less than 0.1% of the bunch crossings occupied; as for ZDC, the correction is completely negligible.

Differences between normalization ratios R_2, R_B and R_Y obtained by ZDC and BBC are presented in fig. 5 for the four dedicated fills. Most important R_2 ratio shows significant systematic shift of $1.4 \cdot 10^{-3}$ at the 4σ statistical level. Similar plots in fig. 6 with wrong spin pattern assigned to the fills demonstrate no effect, but shows significantly worse χ^2. The second test makes us believe that our method is sensitive to the polarization, while the first one leads us to a conclusion that one of the two detectors or both of them have nonzero double spin sensitivity.

3.3 BBC

For further studies we took advantage of the access to the counts of individual BBC tiles, which are connected to the scaler boards 11 and 12. The idea was to select several tile combinations within the BBC arrays which reflect significantly different physics subprocesses and compare their sensitivity to various spin effects. The assumption was made that two (or more) different processes can have the same spin sensitivity only in the case if it is zero in both (or all) of them. In other words, subprocesses can be considered free of spin effects if they give zero difference in corresponding luminosity ratios R_2, R_B, R_Y.

The following 3 tile combinations were selected independently for East and West BBC arrays:

1. BBC $N > 5$ East(West) - 6 or more tiles have hit in the East(West) array and at least one tile is hit in the opposite side (i.e. BBC coincidence bit is present)
2. BBC Inner East(West) - single hit in the East(West) array and it belongs to the inner set of the tiles and the BBC coincidence bit is present. The inner tiles are numbered 0, 3, 4, 8, 11, 12 in fig. 1.
3. BBC Outer East(West) - single hit in the East(West) array and it belongs to the outer set of the tiles and the BBC coincidence bit is present. The outer tiles have numbers 1, 2, 5, 6, 7, 9, 10, 13, 14, 15 in fig. 1.

Combination 1 represents high multiplicity events. The hits are supposed to be widely distributed over the BBC array and one may expect small spin dependence for such processes. The distribution of the number of BBC tiles hit on the east side for the events with BBC coincidence is shown in fig. 7. We see that most of the events produce a high occupancy in BBC. The portion of the events with $N > 5$ is relatively small so that such selection is quite different from total BBC coincidence count. We also remind here that a hit in one of the BBC sides is produced in less than 0.1% of bunch crossings only, thus multiple hits in one arm cannot be attributed to coinciding events from one bunch crossing, but reflect real multiplicity.

Combination 2 corresponds to a single particle in very forward direction, probably the leading particle, going at some small angle to the beam. Subprocess 3 is similar to 2, but the single particle has twice larger angle. Further below it will be shown that these two subprocesses, though look alike, have significantly different single spin effects and thus represent substantially different physics. Commonly to all three, there is no possibility to specify what kind of hit pattern occurs on the opposite side, because the arrays are connected to different scaler boards. Yet the BBC coincidence bit is required by all three combinations.

Using individual tiles from the inner and outer sets one can evaluate the dependence of the spin effects for subprocesses 2 and 3 on the azimuthal angle. Figures 8 and 9 present the difference in R_B and R_Y single spin ratios for single tiles compared to that for the whole BBC coincidence. The geometrical position of the tile defines its azimuthal angle with respect to the horizontal direction.

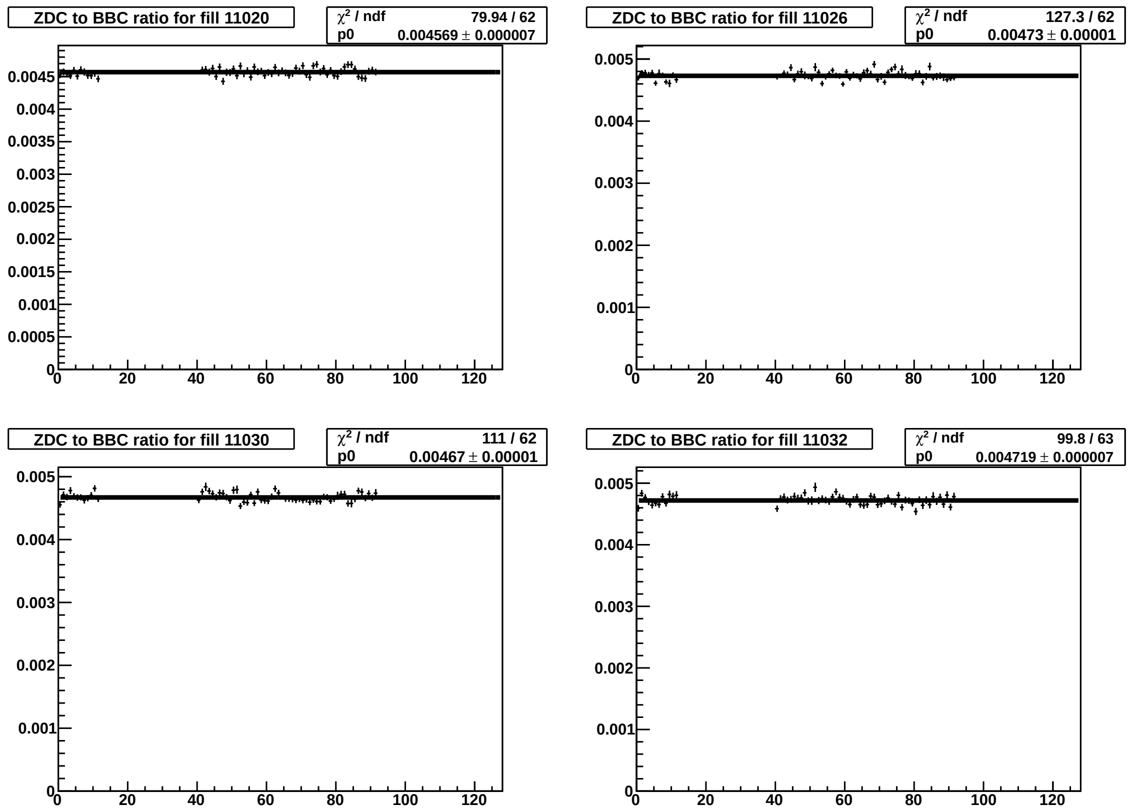

Figure 3: Bunch dependence of ZDC to BBC counts ratio for the 4 pp2pp fills.

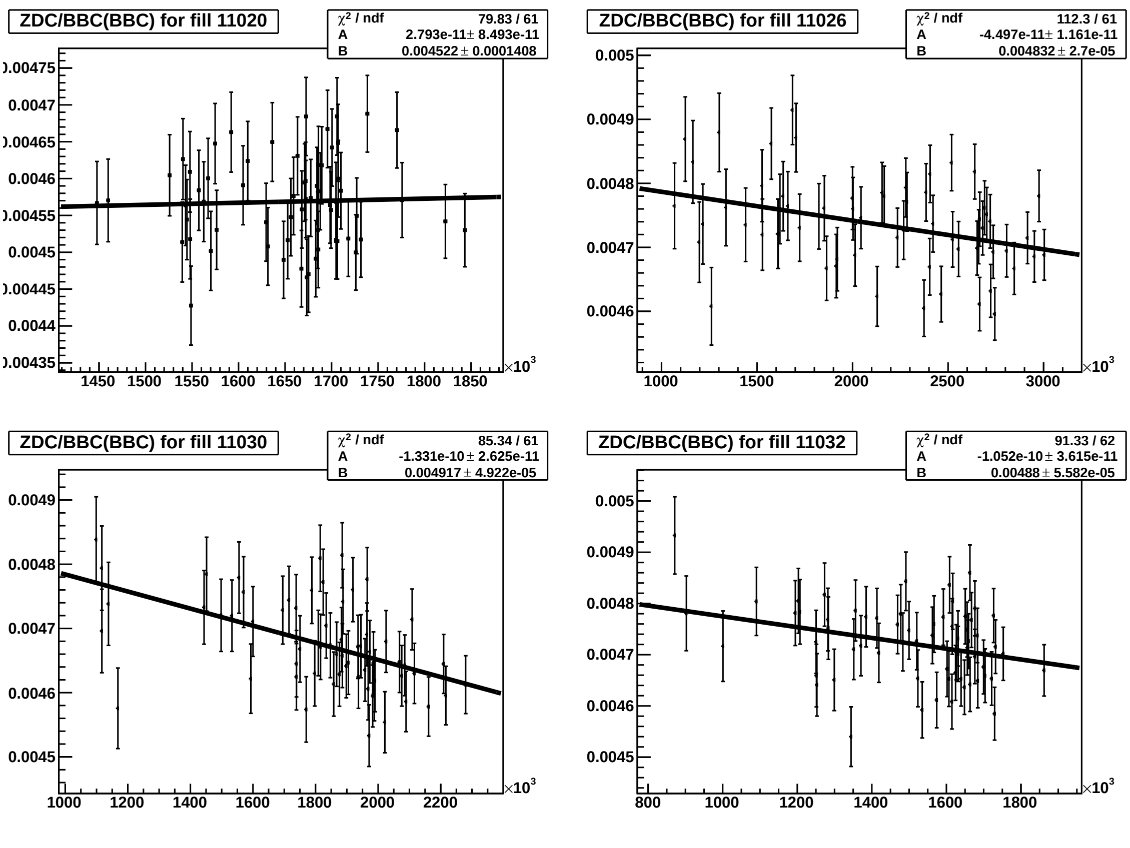

Figure 4: Luminosity dependence of ZDC to BBC counts ratio for the 4 pp2pp fills.

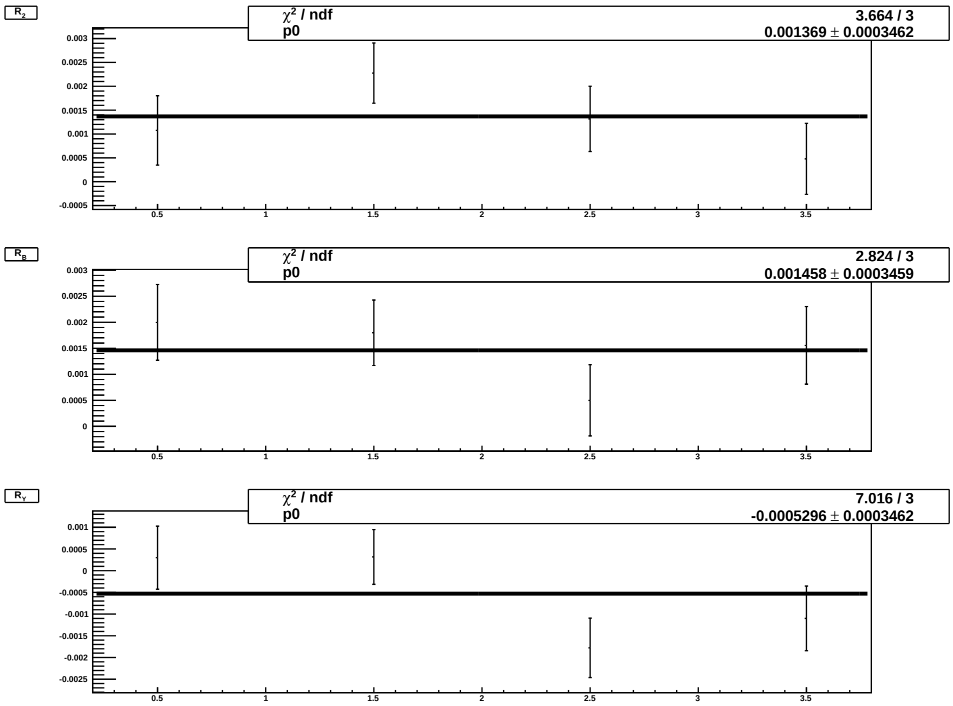

Figure 5: ZDC - BBC difference of R_2, R_B and R_Y.

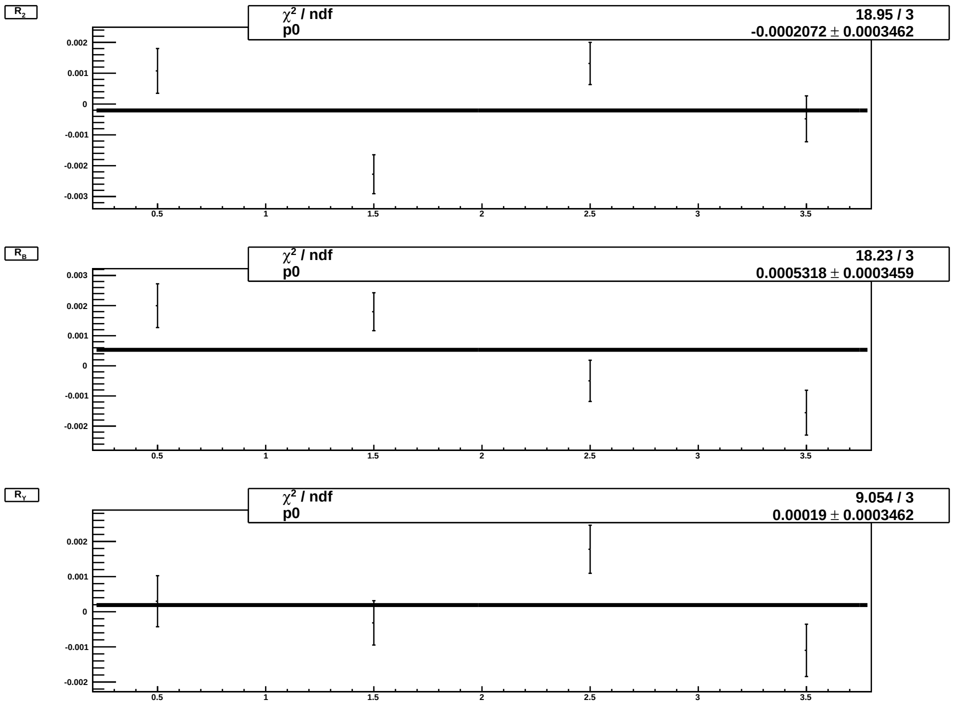

Figure 6: ZDC - BBC difference of R_2, R_B and R_Y for the wrong fill pattern.

For the outer tiles connected to the same scaler channel (pairs numbered 1 and 9) two identical points are shown at the two corresponding angles. The data is averaged over all four of pp2pp low intensity fills. Significant cosine-like effects can be seen for the inner tiles in the corresponding beam fragmentation direction. As expected, this is west for the blue beam and east for the yellow one. No clear dependencies are observed in the opposite directions, which is also expected. For the outer tiles R_B also suggests cosine behavior in the west, but the sign of the effect is opposite to that for the inner tiles. This gives a proof of the fact that the spin dependence of the processes reflected by the hits in the inner and outer tile sets is significantly different. At the same time expected effect for R_Y in the east can not be clearly seen, though can be suspected and with the same sign as for R_B in the west. Similarly to the inner sets, opposite directions show no clear effects. In addition, one can notice small average shifts of the order of $5 \cdot 10^{-4}$ common to all four plots in each of the figures 8 and 9. This should be attributed tho the residual single spin effect in the whole BBC coincidence count, since corresponding R_B and R_Y values are subtracted from those obtained for individual tiles. These residual effects have opposite signs for R_B and R_Y, but are of the same order of magnitude.

Figure 10 presents similar values for the R_2 double spin ratio, which is most important for the extraction of the asymmetries. The points in each plot are fitted with a constant and the χ^2 values do not allow to suspect any angular dependence. Moreover, all shifts are very small (below $1.5 \cdot 10^{-4}$) and comparable with zero within two statistical errors at most. According to our main assumption, we are bound to conclude that subprocesses 2 and 3 as well as the whole BBC coincidence process are free of double spin effects at least at this level.

Unlike single spin effects which are expected to be seen (and were observed) in the forward direction of the corresponding polarized beam, double spin manifestation is supposed to be direction-symmetric because both beams are involved. Left part of figure 11 shows east to west comparison of R_2 normalization ratios for each of the three subprocesses under discussion for the four pp2pp fills. East and west in this case represent the same physics. Low χ^2 and small average differences in all three plots proof this hypothesis and confirms high quality of the data. For the final R_2 uncertainty estimates east and west values were averaged for each subprocess to get better statistical significance.

On the right side of figure 11 the R_2 ratio for the three subprocesses is compared to that of the whole BBC coincidence. The points represent the corresponding difference in R_2 values for the four pp2pp fills and are fitted with a constant. All average differences are small, below $1.1 \cdot 10^{-4}$, and comparable with zero within 2.5 statistical errors in the worst case. Thus we conclude that subprocesses 1, 2, 3 *and* the whole BBC coincidence, though have different physics origin, show the same double spin sensitivity. Therefore all the four have very small double spin effects and any of them can be used for normalization. It is worth mentioning that the three subprocesses share only a small portion of the whole BBC statistics, and thus the latter can be treated as an independent physics process.

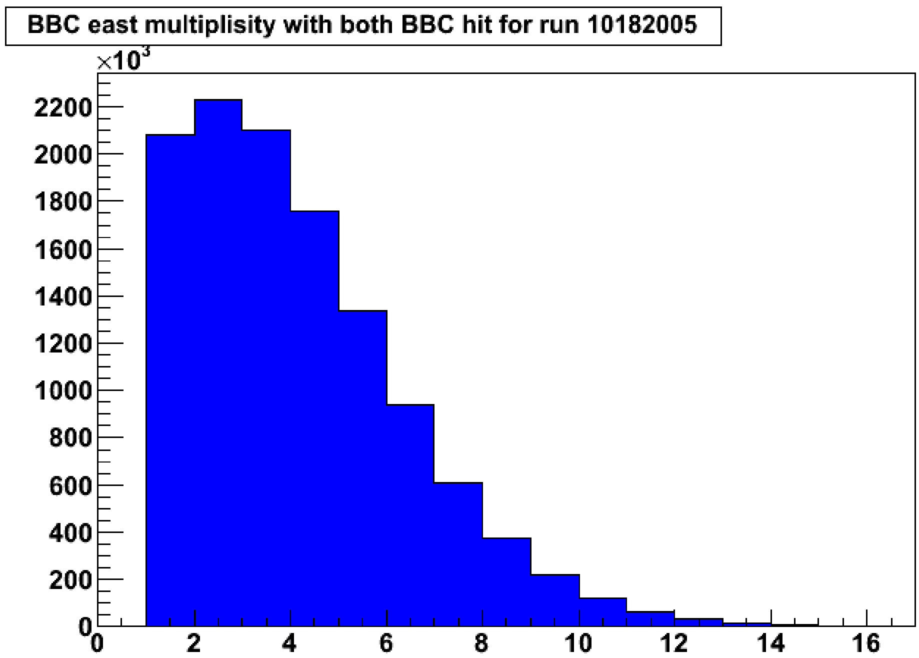

Figure 7: BBC multiplicity.

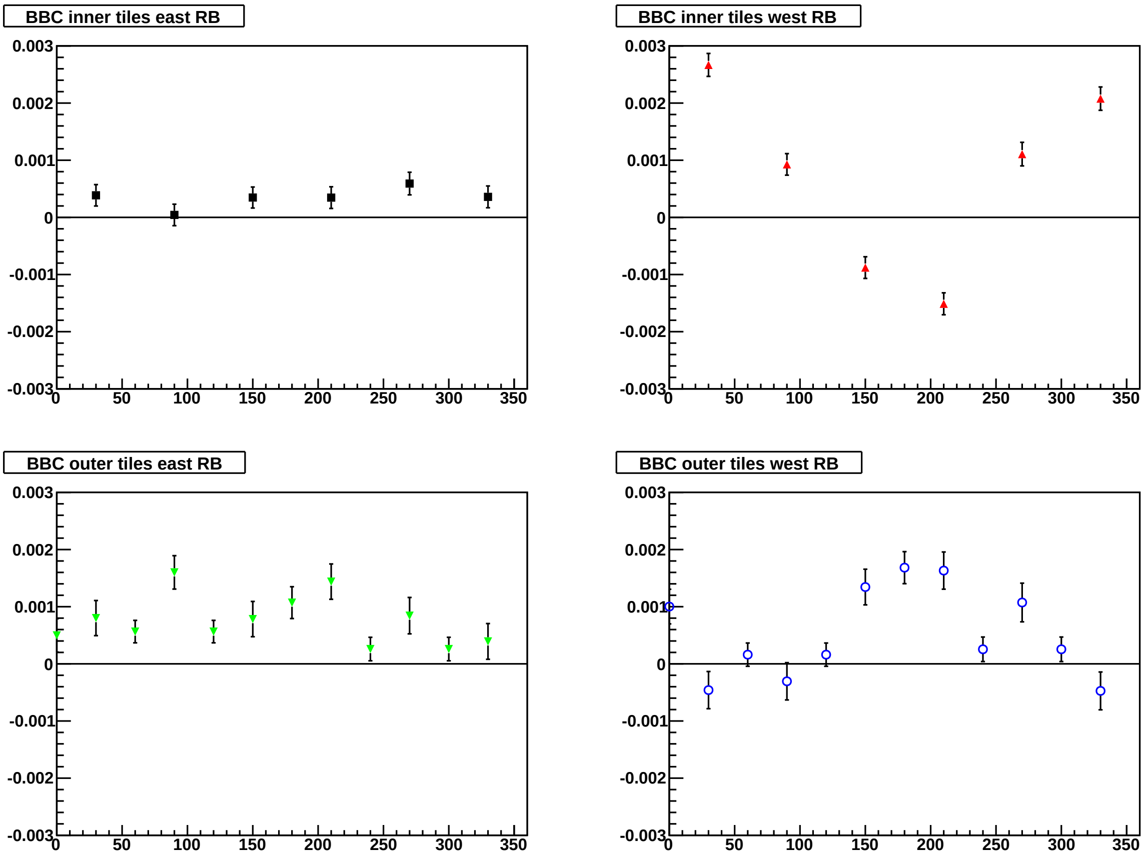

Figure 8: Difference in R_B ratio as a function of the tile azimuthal angle.

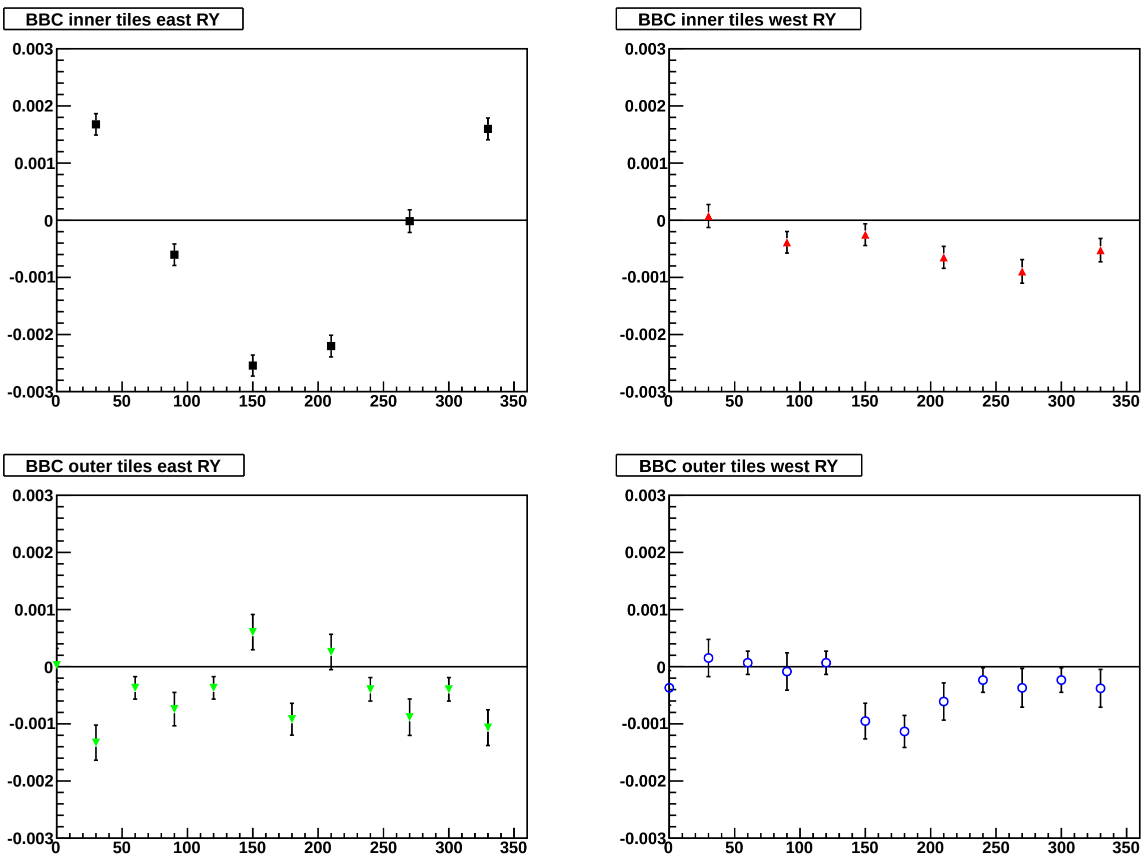

Figure 9: Difference in R_Y ratio as a function of the tile azimuthal angle.

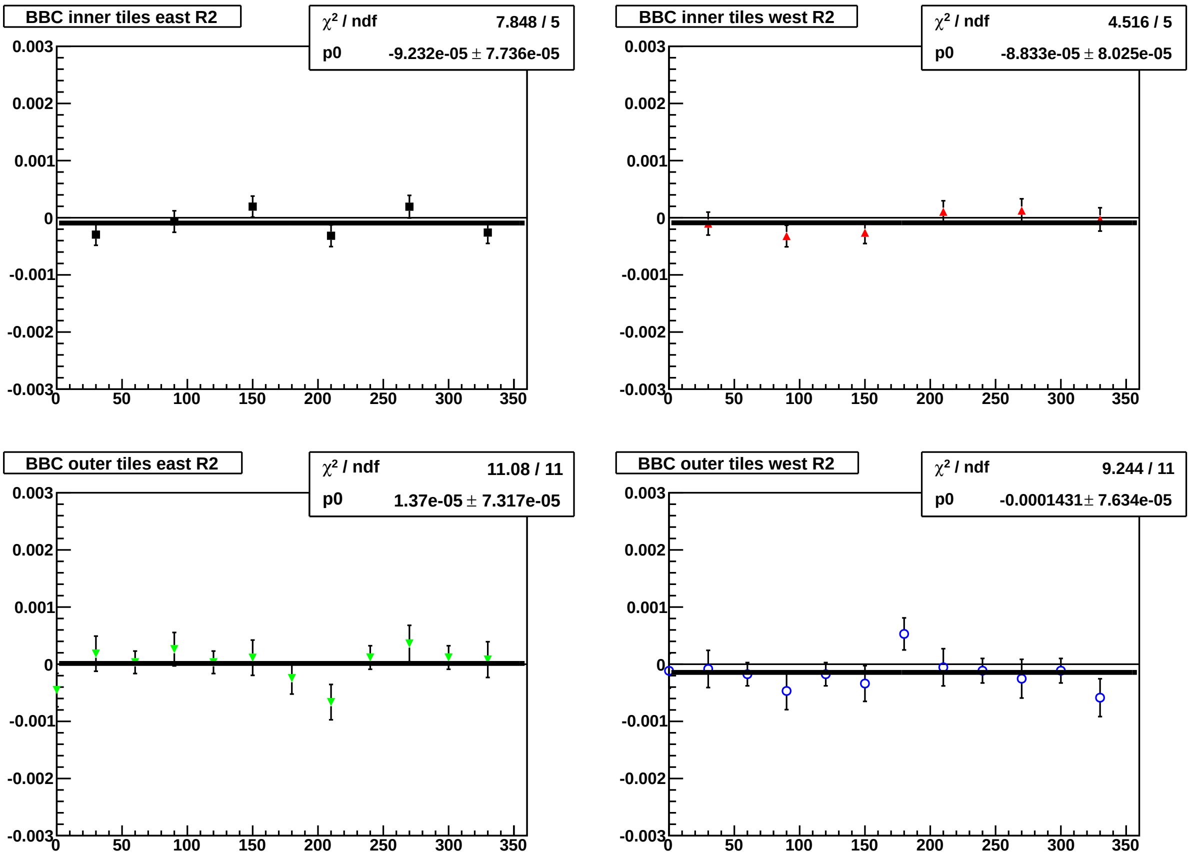

Figure 10: Difference in R_2 ratio as a function of the tile azimuthal angle.

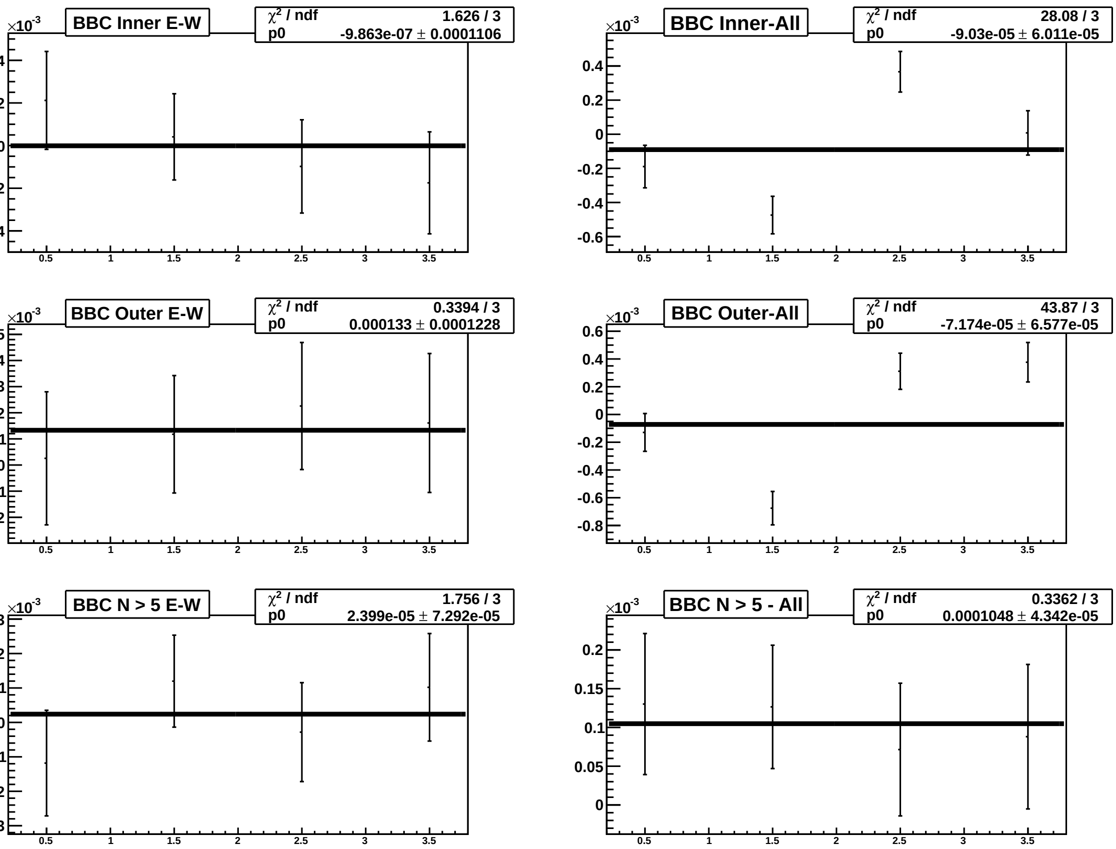

Figure 11: BBC inner, outer and high multiplicity R_2 comparison: left – east to west, right – each of the three to the BBC coincidence.

One can notice (very) large χ^2 values in the two upper right plots. This could be prescribed to the residual effects, originating from the particular fill properties, such as bunch shape variations (see section 3.1). Such effects are beyond our control and, generally, may introduce additional R_2 uncertainty. Yet, fortunately, the averages of the four particular pp2pp fills give very small values, and these particular values should be used for the uncertainty estimates in our case. Nevertheless, such small values are not the general property of BBC as a double spin normalization source, though the uncertainties calculated for each particular case should be expected to be of this order of magnitude.

For the normalization purposes the whole BBC coincidence is the most preferable source because of the two reasons. First, it has significantly higher statistics than any of the three subprocesses discussed. Second, the multiples and accidentals correction as in [1] can be applied to the whole BBC counts. Though the correction is very small for pp2pp running period and its influence on the R_2 ratio is at all negligible, it's better to account for it when we are talking about numbers of the 10^{-4} order of magnitude.

4 Conclusions

Several RHIC and STAR subsystems were analyzed in order to find the best normalization source for double spin asymmetries extraction. VPD excellently performed as a subsystem, but was found to be not enough reliably timed into the general purpose STAR scaler board. RHIC WCM product, though expected to be well spin independent, does not reflect real luminosity because of bunch shape or trajectory variations. Double spin effects of the order $1.4 \cdot 10^{-3}$ have to be attributed to ZDC by comparison to BBC, which was proved to have much smaller double spin sensitivity.

Three subprocesses in the BBC arrays were shown to bear significantly different physics. All three were compared to the whole BBC coincidence and very small difference in R_2 double spin normalization ratio was observed. The conclusion was made that the whole BBC as well as any of the subprocesses are nearly free of double spin effects. The choice of BBC coincidence as the most appropriate normalization source was justified.

To quantify the residual uncertainty in R_2 the deviations from BBC coincidence obtained for three independent physics subprocesses (see fit values in the right plots of figure 11) were used to form the RMS value. The resulting numeric estimate gives $\delta R_2 = 1.56 \cdot 10^{-4}$.

Deep investigation of the normalization influence on the physics observables was performed (see appendix to this note). It was clearly shown that the main and the only source of the systematic error due to the normalization uncertainty is the double spin ratio R_2. The contribution is:

$$\delta \frac{A_{NN} + A_{SS}}{2} = \frac{2}{P_B P_Y} \delta R_2 = 8.4 \cdot 10^{-4}. \tag{2}$$

At the same time the normalization uncertainty in $(A_{NN} - A_{SS})/2$ can be completely neglected compared to the statistical error.

Though we developed good analytic understanding of the normalization uncertainties, we will calculate the derivatives numerically for our particular data set to check the algebraic results.

A Systematic Errors in Raw Double Spin Asymmetries due to Normalization Factors

A.1 General considerations

During the normalization studies for transverse double spin asymmetries in the CNI region, three *independent* normalizing ratios R_2, R_B and R_Y were investigated for several STAR subsystems and their parts, sensitive for different physics processes. The goal of this note is to prove that the systematic error of the raw double spin asymmetry is dominated by the uncertainty in R_2, while the contribution from poorly defined R_B and R_Y is negligibly small.

First define some terms and designations:

N^{++}, N^{--}, N^{+-} and N^{-+} – event numbers obtained for a certain physics process under study for corresponding spin combinations, also sometimes will be referred as N^{BY}, first index for BLUE beam;

L^{++}, L^{--}, L^{+-} and L^{-+} – corresponding event numbers in the system used for normalization, or normalizing counts, also L^{BY};

$L = L^{++} + L^{--} + L^{+-} + L^{-+}$ – is then the total count of the normalizing system;

$r^{BY} = 2L^{BY}/L$ – are twice the relative luminosities of four colliding spin combinations so that $(r^{++} + r^{--} + r^{+-} + r^{-+})/2 = 1$;

$R_2 = (L^{++} + L^{--})/L$ – is the relative part of the parallel spin interactions;

$R_B = (L^{++} + L^{+-})/L$ – is the relative part of the interactions with spin UP in the BLUE beam and

$R_Y = (L^{++} + L^{-+})/L$ – is the relative part of the interactions with spin UP in the YELLOW beam;

the last three ratios are also referred as R_j and it is important, that R_j's are *independent* ratios contrary to r^{BY}'s.

Exact definition of the raw transverse double spin asymmetry is:

$$A_2 = \frac{\left(\frac{N^{++}}{L^{++}} + \frac{N^{--}}{L^{--}}\right) - \left(\frac{N^{+-}}{L^{+-}} + \frac{N^{-+}}{L^{-+}}\right)}{\left(\frac{N^{++}}{L^{++}} + \frac{N^{--}}{L^{--}}\right) + \left(\frac{N^{+-}}{L^{+-}} + \frac{N^{-+}}{L^{-+}}\right)} = \frac{\frac{N^{++}}{r^{++}} + \frac{N^{--}}{r^{--}} - \frac{N^{+-}}{r^{+-}} - \frac{N^{-+}}{r^{-+}}}{\frac{N^{++}}{r^{++}} + \frac{N^{--}}{r^{--}} + \frac{N^{+-}}{r^{+-}} + \frac{N^{-+}}{r^{-+}}} = \frac{D}{S} \tag{3}$$

and we are interested in derivatives $\partial A_2/\partial R_j$ as measures of the contributions of the corresponding ratios to the systematic error.

Note some useful expressions:

$R_2 + R_B + R_Y = 2\frac{L^{++}}{L} + 1$, and thus:

$r^{++} = R_2 + R_B + R_Y - 1$. Further from definitions of R_j's:

$r^{--} = 2(R_2 - \frac{L^{++}}{L}) = R_2 + 1 - R_B - R_Y$

$r^{+-} = 2(R_B - \frac{L^{++}}{L}) = R_B + 1 - R_2 - R_Y$

$r^{-+} = 2(R_Y - \frac{L^{++}}{L}) = R_Y + 1 - R_2 - R_B$

Now going to derivatives from (3):

$$\frac{\partial A_2}{\partial R_j} = \frac{S \cdot \frac{\partial D}{\partial R_j} - D \cdot \frac{\partial S}{\partial R_j}}{S^2} = \frac{\frac{\partial D}{\partial R_j} - A_2 \cdot \frac{\partial S}{\partial R_j}}{S} \tag{4}$$

In turn,

$$\begin{aligned}
\frac{\partial D}{\partial R_j} &= \frac{\partial D}{\partial r^{++}} \cdot \frac{\partial r^{++}}{\partial R_j} + \frac{\partial D}{\partial r^{--}} \cdot \frac{\partial r^{--}}{\partial R_j} + \frac{\partial D}{\partial r^{+-}} \cdot \frac{\partial r^{+-}}{\partial R_j} + \frac{\partial D}{\partial r^{-+}} \cdot \frac{\partial r^{-+}}{\partial R_j} = \\
&= -\left(\frac{N^{++}}{(r^{++})^2} \cdot \frac{\partial r^{++}}{\partial R_j} + \frac{N^{--}}{(r^{--})^2} \cdot \frac{\partial r^{--}}{\partial R_j} - \frac{N^{+-}}{(r^{+-})^2} \cdot \frac{\partial r^{+-}}{\partial R_j} - \frac{N^{-+}}{(r^{-+})^2} \cdot \frac{\partial r^{-+}}{\partial R_j} \right) \qquad (5) \\
\frac{\partial S}{\partial R_j} &= -\left(\frac{N^{++}}{(r^{++})^2} \cdot \frac{\partial r^{++}}{\partial R_j} + \frac{N^{--}}{(r^{--})^2} \cdot \frac{\partial r^{--}}{\partial R_j} + \frac{N^{+-}}{(r^{+-})^2} \cdot \frac{\partial r^{+-}}{\partial R_j} + \frac{N^{-+}}{(r^{-+})^2} \cdot \frac{\partial r^{-+}}{\partial R_j} \right) \qquad (6)
\end{aligned}$$

Taking into account that all $\partial r^{BY}/\partial R_j$ are either $+1$ or -1, produce explicit expressions:

$$\begin{aligned}
-\frac{\partial D}{\partial R_2} &= \frac{N^{++}}{(r^{++})^2} + \frac{N^{--}}{(r^{--})^2} + \frac{N^{+-}}{(r^{+-})^2} + \frac{N^{-+}}{(r^{-+})^2} && (7) \\
-\frac{\partial D}{\partial R_B} &= \frac{N^{++}}{(r^{++})^2} - \frac{N^{--}}{(r^{--})^2} - \frac{N^{+-}}{(r^{+-})^2} + \frac{N^{-+}}{(r^{-+})^2} && (8) \\
-\frac{\partial D}{\partial R_Y} &= \frac{N^{++}}{(r^{++})^2} - \frac{N^{--}}{(r^{--})^2} + \frac{N^{+-}}{(r^{+-})^2} - \frac{N^{-+}}{(r^{-+})^2} && (9) \\
-\frac{\partial S}{\partial R_2} &= \frac{N^{++}}{(r^{++})^2} + \frac{N^{--}}{(r^{--})^2} - \frac{N^{+-}}{(r^{+-})^2} - \frac{N^{-+}}{(r^{-+})^2} && (10) \\
-\frac{\partial S}{\partial R_B} &= \frac{N^{++}}{(r^{++})^2} - \frac{N^{--}}{(r^{--})^2} + \frac{N^{+-}}{(r^{+-})^2} - \frac{N^{-+}}{(r^{-+})^2} && (11) \\
-\frac{\partial S}{\partial R_Y} &= \frac{N^{++}}{(r^{++})^2} - \frac{N^{--}}{(r^{--})^2} - \frac{N^{+-}}{(r^{+-})^2} + \frac{N^{-+}}{(r^{-+})^2} && (12)
\end{aligned}$$

With RHIC running conditions in the first approximation $r^{++} \approx r^{--} \approx r^{+-} \approx r^{-+} \approx r = 1/2$. In addition, all asymmetries are very small: $A_N \sim 10^{-2}$ and $A_{NN} \sim A_{SS} \sim 10^{-3}$, which means $N^{++} \approx N^{--} \approx N^{+-} \approx N^{-+} \approx N$. In this assumption all derivatives (8)-(12) approximately evaluate to 0 except for (7): $\frac{\partial D}{\partial R_2} \approx -4N/r^2$.

Returning to (4) note that if even our assumption is not completely true, the second term in the numerator can be totally neglected for all j since it is additionally suppressed by the small factor A_2 and all $\frac{\partial S}{\partial R_j}$ are close to zero. Naturally the statement holds within our approximation framework. Then evaluating $S \approx 4N/r$, we have:

$$\frac{\partial A_2}{\partial R_2} \approx -1/r = -2\ ; \qquad \frac{\partial A_2}{\partial R_B} \approx \frac{\partial A_2}{\partial R_Y} \approx 0\ . \tag{13}$$

To probe next to leading order behavior of this result, let us now assume that, as before, all r^{BY} are approximately equal, but the single spin asymmetry A_N is not negligible. We will concentrate on $\frac{\partial A_2}{\partial R_B}$ since all conclusions below will be very similar for $\frac{\partial A_2}{\partial R_Y}$ while $\frac{\partial A_2}{\partial R_2}$ will not undergo any significant changes. Then with the above assumption:

$$-\frac{\partial D}{\partial R_B} = \left(\frac{N^{++}}{r^2} - \frac{N^{+-}}{r^2} \right) + \left(\frac{N^{-+}}{r^2} - \frac{N^{--}}{r^2} \right) =$$

$$= \frac{1}{r}\left(A_Y \cdot \left(\frac{N^{++}}{r}+\frac{N^{+-}}{r}\right)+A_Y \cdot \left(\frac{N^{-+}}{r}+\frac{N^{--}}{r}\right)\right)=\frac{A_Y}{r}\cdot S\,,\text{ where}$$

$$A_Y=\frac{\frac{N^{++}}{r^{++}}-\frac{N^{+-}}{r^{+-}}}{\frac{N^{++}}{r^{++}}+\frac{N^{+-}}{r^{+-}}}=\frac{\frac{N^{-+}}{r^{-+}}-\frac{N^{--}}{r^{--}}}{\frac{N^{-+}}{r^{-+}}+\frac{N^{--}}{r^{--}}} \tag{14}$$

is the raw single spin asymmetry with the YELLOW beam and thus

$$\frac{\partial A_2}{\partial R_B}=-\frac{A_Y}{r}=-2\cdot A_Y\,, \tag{15}$$

which makes maximum 0.03 of $\frac{\partial A_2}{\partial R_2}$ with measured values of A_N. Similarly, $\frac{\partial A_2}{\partial R_Y}$ will relate in the same way to A_B, the single spin asymmetry with the BLUE beam.

Another estimate is based on the assumption that, contrary to the previous one, $A_N = A_{NN} = A_{SS} = 0$, but r^{BY}'s are different. In this case N^{BY} is strictly proportional to r^{BY}: $N^{BY} = C \cdot r^{BY}$ and we have:

$$-\frac{\partial D}{\partial R_B} = C\cdot\left(\frac{1}{r^{++}}-\frac{1}{r^{--}}-\frac{1}{r^{+-}}+\frac{1}{r^{-+}}\right)$$

$$S = 4\cdot C\,,\text{and}$$

$$\begin{aligned}\frac{\partial A_2}{\partial R_B} &= -\frac{1}{4}\cdot\left(\frac{1}{r^{++}}-\frac{1}{r^{--}}-\frac{1}{r^{+-}}+\frac{1}{r^{-+}}\right)\approx\\ &\approx -\frac{1}{4r}\cdot\left(\left(1-\frac{\Delta r^{++}}{r}\right)-\left(1-\frac{\Delta r^{--}}{r}\right)-\left(1-\frac{\Delta r^{+-}}{r}\right)+\left(1-\frac{\Delta r^{-+}}{r}\right)\right)=\\ &= -\frac{1}{4r}\cdot\left(\frac{\Delta r^{++}}{r}-\frac{\Delta r^{--}}{r}-\frac{\Delta r^{+-}}{r}+\frac{\Delta r^{-+}}{r}\right)\end{aligned} \tag{16}$$

where Δr^{BY} is the deviation of r^{BY} from its average value of $r = 1/2$. A good numeric estimate would arise if we consider the case of 'one bunch missing', that is, with 64 colliding bunches, means that $\Delta r^{BY}/r^{BY} = -\Delta r/r = -0.06$ for the missing spin combination and $\Delta r^{BY}/r^{BY} = \Delta r/3r = 0.02$ for all three other ones:

$$\frac{\partial A_2}{\partial R_B}=-\frac{1}{4r}\cdot\left(\pm\frac{4}{3}\cdot\frac{\Delta r}{r}\right)=\pm\frac{2}{3}\cdot\frac{\Delta r}{r}\,, \tag{17}$$

where the sign depends on which particular spin combination is missing. Numerically this is 0.02 of $\frac{\partial A_2}{\partial R_2}$. As for $\frac{\partial A_2}{\partial R_Y}$, it will have the same value but either the same or different sign as $\frac{\partial A_2}{\partial R_B}$, again dependent on the missing combination.

As it was found during the normalization studies, the uncertainty δR_B and δR_Y is approximately 5 times larger than δR_2. Nevertheless taking into account the small estimated values of derivatives for the two single beam ratios, their influence on the resulting systematic error can be neglected when added in quadratures according to general formula:

$$\delta A_2=\sqrt{\left(\delta R_2\cdot\frac{\partial A_2}{\partial R_2}\right)^2+\left(\delta R_B\cdot\frac{\partial A_2}{\partial R_B}\right)^2+\left(\delta R_Y\cdot\frac{\partial A_2}{\partial R_Y}\right)^2} \tag{18}$$

Concluding, the systematic error in the raw transverse double spin asymmetry can be safely calculated taking into account only the uncertainty in the R_2 normalization ratio and completely disregarding the poor knowledge of R_B and R_Y:

$$\delta A_2 = 2\cdot\delta R_2 \tag{19}$$

A.2 Physics Asymmetries

All the above considerations are directly applicable to the uncertainty in the value of the raw physics asymmetry $A_{2+} = P_B P_Y (A_{NN} + A_{SS})/2$. Indeed, the initial equation (3) can be treated as a relation at a certain azimuthal angle φ and in this case $A_2(\varphi)$, $N^{BY}(\varphi)$, $D(\varphi)$, $S(\varphi)$ should be considered as functions of this angle. Naturally all the consequent results will hold for this particular φ, and thus for any φ in the range $[0; 2\pi]$ of the measurement. The manifestation of A_{2+} does not have any angular dependence (see (21) below) and can be calculated as an average of $A_2(\varphi)$ over this range. Consequently all the above results will stay true if considered as averages over φ. Particularly, equations (13), (17) will not change, while (15) will average out to zero, making the result (19) even better justified. And thus

$$\delta A_{2+} = 2 \cdot \delta R_2. \tag{20}$$

The situation is completely different when it comes to the physics asymmetry $A_{2-} = P_B P_Y (A_{NN} - A_{SS})/2$. The raw double spin asymmetry $A_2(\varphi)$ can be expressed as:

$$A_2(\varphi) = A_{2+} + A_{2-} \cos 2\varphi, \tag{21}$$

so that A_{2+} is effectively a cross-section difference for different spin combinations, showing up as a constant term in A_2, while A_{2-} is the asymmetry variation with azimuthal angle and can be extracted by fitting A_2 with a $\cos 2\varphi$ function. A rough estimate of A_{2-} can be obtained from the following relation:

$$A_{2-} = \frac{1}{2}\left(\frac{(A_2(0) - A_2(\pi/2)) + (A_2(\pi) - A_2(3\pi/2))}{2}\right). \tag{22}$$

Since uncertainty (19) is angular independent and thus totally correlated for all angular dependent terms in (22), its obvious from the structure of this expression that the uncertainty of A_{2-} is zero in the leading approximation:

$$\delta A_{2-} \approx 0. \tag{23}$$

A.3 Uncertainties in $(A_{NN} - A_{SS})/2$

Nevertheless, for better understanding, we will try to estimate next to leading order behavior of A_{2-} uncertainty using (22). This expression is intentionally written in the angular-symmetric form in order to suppress the remains of single spin effects, as will be seen from the following. As in section A.1 we will calculate derivatives $\frac{\partial A_{2-}}{\partial R_j}$. Let us designate

$$H_1 = A_2(0) - A_2(\pi/2),\ H_2 = A_2(\pi) - A_2(3\pi/2), \quad \text{so that} \quad \frac{\partial A_{2-}}{\partial R_j} = \frac{1}{4}\left(\frac{\partial H_1}{\partial R_j} + \frac{\partial H_2}{\partial R_j}\right) \tag{24}$$

and we will concentrate on the first term of (24) and on its derivative over R_2.

We will express equation (7) and the denominator S of (3) in the form of sums:

$$-\frac{\partial D}{\partial R_2}(\varphi) = \sum_{B,Y=+,-}^{(4)} \frac{N^{BY}(\varphi)}{(r^{BY})^2}, \qquad S(\varphi) = \sum_{B,Y=+,-}^{(4)} \frac{N^{BY}(\varphi)}{r^{BY}}, \tag{25}$$

where summation goes over all 4 beam spin combinations and the numbers in parentheses on top of the sum symbols denote the total number of terms in each sum.

Neglecting second term in (4) and substituting (25):

$$\frac{\partial H_1}{\partial R_2} \;=\; \frac{\partial A_2}{\partial R_2}(0) - \frac{\partial A_2}{\partial R_2}(\pi/2) \;=\; \frac{\frac{\partial D}{\partial R_2}(0)}{S(0)} - \frac{\frac{\partial D}{\partial R_2}(\pi/2)}{S(\pi/2)} \;=$$

$$= \frac{\sum\limits_{B,Y=+,-}^{(4)} \frac{N^{BY}(\pi/2)}{(r^{BY})^2}}{\sum\limits_{B,Y=+,-}^{(4)} \frac{N^{BY}(\pi/2)}{r^{BY}}} - \frac{\sum\limits_{b,y=+,-}^{(4)} \frac{N^{by}(0)}{(r^{by})^2}}{\sum\limits_{b,y=+,-}^{(4)} \frac{N^{by}(0)}{r^{by}}} =$$

$$= \frac{\sum\limits_{B,Y,b,y=+,-}^{(16)} \frac{N^{BY}(\pi/2)}{(r^{BY})^2}\cdot\frac{N^{by}(0)}{r^{by}} - \frac{N^{by}(0)}{(r^{by})^2}\cdot\frac{N^{BY}(\pi/2)}{r^{BY}}}{S(0)S(\pi/2)} =$$

$$= \frac{\sum\limits_{B,Y,b,y=+,-}^{(16)} \frac{N^{BY}(\pi/2)N^{by}(0)}{(r^{BY}r^{by})^2}(r^{by}-r^{BY})}{S(0)S(\pi/2)}. \tag{26}$$

Note that 4 terms in (26) with $BY = by$ equal zero because $r^{by} = r^{BY}$ in these cases. The remaining 12 elements can be grouped in pairs combining $BYby$ and $byBY$ terms to obtain:

$$\frac{\partial H_1}{\partial R_2} = \frac{\sum\limits_{B,Y,b,y=+,-}^{(6)} \frac{N^{BY}(\pi/2)N^{by}(0)-N^{BY}(0)N^{by}(\pi/2)}{(r^{BY}r^{by})^2}(r^{by}-r^{BY})}{S(0)S(\pi/2)}, \tag{27}$$

where combinations of spin indices run over the following set of actual values: $(BYby) = \{(++ +-), (++-+), (++--), (+--+), (+---), (-+--)\}$.

For these 6 remaining terms one can write out explicit expressions using the common formula:

$$\begin{aligned} N^{by}(\varphi) &= N_0^{by}C(\varphi)(1 + A_N(P_B+P_Y)\cos\varphi + P_BP_Y(A_{NN}+A_{SS})/2 + P_BP_Y(A_{NN}-A_{SS})/2\cos 2\varphi) = \\ &= N_0^{by}C(\varphi)(1 + (b\cdot A_B + y\cdot A_Y)\cos\varphi + b\cdot y\cdot A_{2+} + b\cdot y\cdot A_{2-}\cos 2\varphi), \end{aligned} \tag{28}$$

where $C(\varphi)$ represents the setup acceptance at this azimuthal angle and b, y are either $+$ or $-$. Omitting terms quadratic in asymmetries in the products, and noting, that $N_0^{by}C(\varphi)$ are the leading terms in corresponding $N^{by}(\varphi)$, we obtain:

$$\begin{aligned} \frac{\partial H_1}{\partial R_2} = \frac{1}{S(0)S(\pi/2)}[\; & \frac{N^{++}(\pi/2)N^{+-}(0)(r^{++}-r^{+-})}{(r^{++}r^{+-})^2}(-2A_Y - 4A_{2-}) \; + \\ + \; & \frac{N^{++}(\pi/2)N^{-+}(0)(r^{++}-r^{-+})}{(r^{++}r^{-+})^2}(-2A_B - 4A_{2-}) \; + \\ + \; & \frac{N^{++}(\pi/2)N^{--}(0)(r^{++}-r^{--})}{(r^{++}r^{--})^2}(-2(A_B + A_Y)) \; + \\ + \; & \frac{N^{+-}(\pi/2)N^{-+}(0)(r^{+-}-r^{-+})}{(r^{+-}r^{-+})^2}(-2(A_B - A_Y)) \; + \\ + \; & \frac{N^{+-}(\pi/2)N^{--}(0)(r^{+-}-r^{--})}{(r^{+-}r^{--})^2}(-2A_B + 4A_{2-}) \; + \\ + \; & \frac{N^{-+}(\pi/2)N^{--}(0)(r^{-+}-r^{--})}{(r^{-+}r^{--})^2}(-2A_Y + 4A_{2-}) \;] \end{aligned} \tag{29}$$

Following the same procedure for H_2, we obtain very similar relation for $\frac{\partial H_2}{\partial R_2}$, except that all A_B and A_Y terms have opposite signs. This becomes clear from (28): $N^{by}(3\pi/2) = N^{by}(\pi/2)$, while $N^{by}(\pi)$ only differs from $N^{by}(0)$ by the sign of the single spin terms.

Now, for all variables, that do not contain any smallness, we can substitute their approximate values, using the assumption $r^{++} \approx r^{--} \approx r^{+-} \approx r^{-+} \approx r = 1/2$ and $N^{++} \approx N^{--} \approx N^{+-} \approx N^{-+} \approx N$. Mind, that we can safely do this because the acceptance products $C(\varphi)C(\varphi+\pi/2)$ which may dominate in the angular dependence of $N^{by}(\varphi)N^{BY}(\varphi+\pi/2)$ are implicitly present in the denominator product of $S(\varphi)S(\varphi+\pi/2)$ and thus completely cancel out.

Adding then the two halves of (24), the single spin terms go away and we obtain the following:

$$\frac{\partial A_{2-}}{\partial R_2} = -\frac{A_{2-}}{2}[(r^{++} - r^{+-}) + (r^{++} - r^{-+}) - (r^{+-} - r^{--}) - (r^{-+} - r^{--})] \tag{30}$$

or, after some conversions:

$$\frac{\partial A_{2-}}{\partial R_2} = -4A_{2-}(R_2 - \frac{1}{2}) \tag{31}$$

The obtained value, though is not exactly zero, is very small, since it contains a product of small numbers: $A_{2-} \sim 10^{-3}$ and $(R_2) - 1/2 \sim 10^{-2}$. Obviously the error in A_{2-} produced by R_2 uncertainty is much lower than the statistical error and can be totally neglected.

Next we'll address the issue of $\frac{\partial A_{2-}}{\partial R_B}$. For this we reword (8) in the form:

$$-\frac{\partial D}{\partial R_B} = \sum_{b,y=+,-}^{(4)} y \frac{N^{by}}{(r^{by})^2}, \tag{32}$$

where y is the sign of the polarization in the yellow beam. Tracing the sign y through the procedure similar to that for $\frac{\partial A_{2-}}{\partial R_2}$, one will realize, that the only dissimilarity is that in (26), (27) instead of $(r^{by} - r^{BY})$ we will have $(Y \cdot r^{by} - y \cdot r^{BY})$. All the consequent reasoning holds and at the end we appear with:

$$\frac{\partial A_{2-}}{\partial R_B} = -\frac{A_{2-}}{2}[(-r^{++} - r^{+-}) + (r^{++} - r^{-+}) - (-r^{+-} + r^{--}) - (-r^{-+} - r^{--})] = 0. \tag{33}$$

Exactly the same result can be obtained very similarly for the third independent derivative:

$$\frac{\partial A_{2-}}{\partial R_Y} = 0. \tag{34}$$

Thus the conclusion is that the single spin ratios R_B, R_Y do not influence the result on A_{2-} even in the next to leading order approximation.

A.4 Normalization uncertainty summary

The following table summarizes the obtained results for the partial derivatives of raw physics asymmetries on the three normalization ratios.

Observable	$\frac{\partial}{\partial R_2}$ LO	$\frac{\partial}{\partial R_2}$ NLO	$\frac{\partial}{\partial R_B}$ LO	$\frac{\partial}{\partial R_B}$ NLO	$\frac{\partial}{\partial R_2}$ LO	$\frac{\partial}{\partial R_2}$ NLO
$A_{2+} = P_B P_Y (A_{NN} + A_{SS})/2$	-2	–	0	$\pm\frac{2}{3} \cdot \frac{\Delta r}{r}$	0	$\pm\frac{2}{3} \cdot \frac{\Delta r}{r}$
$A_{2-} = P_B P_Y (A_{NN} - A_{SS})/2$	0	$-4A_{2-}(R_2 - \frac{1}{2})$	0	0	0	0

It's obvious from the table as well as from the estimates in the above sections that the only normalization uncertainty deserving being accounted as the source of the systematic error to the physics asymmetries is δR_2 and

$$\delta[P_B P_Y (A_{NN} + A_{SS})/2] \approx 2 \cdot \delta R_2, \qquad \text{while} \quad \delta[P_B P_Y (A_{NN} - A_{SS})/2] \approx 0. \tag{35}$$

References

[1] James Hays-Wehle, Joe Seele, Hal Spinka, Bernd Surrow. *Relative Luminosity Analysis for run9 pp 200 GeV Running.* June 26, 2012, Version 0.4

[2] http://www.star.bnl.gov/public/trg/TSL/Schematics/TRG420.pdf